Curcumin-loaded nanocomplexes alleviate the progression of fluke-related cholangiocarcinoma in hamsters

Chanakan Jantawong[1,2], Yaovalux Chamgramol[2,3], Kitti Intuyod[2,3], Aroonsri Priprem[4], Chawalit Pairojkul[2,3], Sirinapha Klungsaeng[5], Rungtiwa Dangtakot[6], Thatsanapong Pongking[1,7], Chutima Sitthirach[5], Porntip Pinlaor[2,7], Sakda Waraasawapati[2,3] and Somchai Pinlaor[2,5*]

*Correspondence:
psomec@kku.ac.th

[1] Biomedical Science Program, Graduate School, Khon Kaen University, Khon Kaen 40002, Thailand
[2] Cholangiocarcinoma Research Institute, Faculty of Medicine, Khon Kaen University, Khon Kaen 40002, Thailand
[3] Department of Pathology, Faculty of Medicine, Khon Kaen University, Khon Kaen 40002, Thailand
[4] Faculty of Pharmacy, Mahasarakham University, Maha Sarakham 44150, Thailand
[5] Department of Parasitology, Faculty of Medicine, Khon Kaen University, Khon Kaen 40002, Thailand
[6] Department of Medical Technology, Faculty of Allied Health Sciences, Nakhonratchasima College, Nakhon Ratchasima 30000, Thailand
[7] Centre for Research and Development in Medical Diagnostic Laboratory, Faculty of Associated Medical Sciences, Khon Kaen University, Khon Kaen 40002, Thailand

Abstract

Background: Curcumin-loaded nanocomplexes (CNCs) previously demonstrated lower toxicity and extended release better than is the case for free curcumin. Here, we evaluated the efficacy of CNCs against opisthorchiasis-associated cholangiocarcinoma (CCA) in hamsters.

Method: Dose optimization (dose and frequency) was performed over a 1-month period using hamsters, a model that is widely used for study of opisthorchiasis-associated cholangiocarcinoma. In the main experimental study, CCA was induced by a combination of fluke, *Opisthorchis viverrini* (OV), infection and *N*-nitrosodimethylamine (NDMA) treatment. Either blank (empty) nanocomplexes (BNCs) or different concentrations of CNCs (equivalent to 10 and 20 mg cur/kg bw) were given to hamsters thrice a week for 5 months. The histopathological changes, biochemical parameters, and the expression of inflammatory/oncogenic transcription factors were investigated. In addition, the role of CNCs in attenuating CCA genesis, as seen in an animal model, was also confirmed in vitro using CCA cell lines.

Results: The optimization study revealed that treatment with CNCs at a dose equivalent to 10 mg cur/kg bw, thrice a week for 1 month, led to a greater reduction of inflammation and liver injury induced in hamsters by OV + NDMA than did treatments at other dose rates. Oral administration with CNCs (10 mg cur/kg bw), thrice a week for 5 months, significantly increased survival rate, reduced CCA incidence, extent of tumor development, cholangitis, bile duct injury and cholangiofibroma. In addition, this treatment decreased serum ALP and ALT activities and suppressed expression of NF-κB, FOXM1, HMGB1, PCNA and formation of 8-nitroguanine. Treatment of CCA cell lines with CNCs also reduced cell proliferation and colony formation, similar to those treated with NF-κB and/or FOXM1 inhibitors.

Conclusion: CNCs (10 mg cur/kg bw) attenuate the progression of fluke-related CCA in hamsters partly via a NF-κB and FOXM1-mediated pathway.

Keywords: Nano-encapsulated curcumin, *Opisthorchis viverrini*, Bile duct cancer, Cholangiofibrosis, Cholangiofibroma, NF-κB and FOXM1

Background

Cholangiocarcinoma (CCA), a primary carcinoma of the intrahepatic bile duct, is generally a rare cancer. However, it has been frequently reported among oriental populations who are endemically infected with the liver flukes, *Opisthorchis viverrini* (OV) (Waraasawapati et al. 2021) or *Clonorchis sinensis*, in parts of the Greater Mekong Sub-region countries (Shin et al. 2010; Sirica et al. 2019). Northeast Thailand has the highest risk of all, with an annual incidence rate of 90 per 100,000 person-years in males and 38.3 per 100,000 person-years in females (Sriamporn et al. 2004). In Northeast Thailand, OV infection is acquired by eating popular simple dishes; marinated chopped raw fish or short-pickled fish, preparations from freshwater fish which contains the infective stage of OV in their tissues (Prueksapanich et al. 2018). Moreover, people in northeastern Thailand are also exposed to a carcinogen (i.e., nitrosamine) in popular fermented fish (Mitacek et al. 1999). Thus, traditional eating habits on a daily basis result in a local population repeatedly exposed to both OV infection and nitrosamine-contaminated food from early in life.

Synergistic effects of nitrosamines and OV infection induce CCA in Syrian golden hamsters, whereas the administration of chemical carcinogen or fluke infection alone does not cause cancer (Thamavit et al. 1987). In this carcinogenesis model, chronic inflammation in response to chronic infestation by liver flukes results in release of cytokines and growth factors leading to biliary cell proliferation (Sripa et al. 2018; van Tong et al. 2017; Yongvanit et al. 2012). At the same time, nitrosamines act as xenobiotics and stimulate hyperplasia of oval cells (hepatic stem/progenitor cells) and cause atypical ductular proliferation. Chronic injury leads to ductular reaction and eventually proliferation and differentiation of oval cells located at canals of Hering, to replace damaged cells (Michalopoulos and Bhushan 2021; Sato et al. 2019). Ductular reaction also activates hepatic stellate cells to become myofibroblasts, which may lead to fibrogenesis (Higashi et al. 2017). These events, along with genetic damage caused by the carcinogen as well as chronic inflammation, may promote cholangiofibrosis, cholangiofibroma (Lee et al. 1997; Ozaki et al. 2021) and development of hepatocellular and/or cholangiocarcinoma (Guest et al. 2017). Based on case series, epidemiological data, and experimental animal models, the International Agency for Research on Cancer has classified OV and *C. sinensis* as class 1 carcinogens in humans (IARC 2012).

Oncogenesis of liver fluke-associated CCA is initiated by molecules derived from oxidation/nitration-derived DNA damage, e.g., 8-nitroguanine (8-NG) and 8-hydroxydeoxyguanosine (8-oxodG) (Banales et al. 2020; Pinlaor et al. 2005; Yongvanit et al. 2012). Upregulation of inflammation-associated transcription factors, e.g., nuclear factor kappa (NF-κB) and activator protein 1 (AP-1), as well as their downstream targets such as inducible nitric oxide synthase (iNOS) and cyclooxygenase-2 (COX-2), have been identified both in animal models (Prakobwong et al. 2010) and clinical samples (Pinlaor et al. 2005). Upregulation of NF-κB (Dolcet et al. 2005), forkhead box m1 (FOXM1) (Wierstra 2013) and high mobility group box 1 (HMGB1) (Vijayakumar et al. 2019) are involved in inflammation-associated carcinogenesis and targeted for cancer therapy. Hence, discovery of agents that exert anti-inflammatory and anti-infection effects and that can attenuate cholangiofibrosis could lead to alternative treatments for CCA.

Compounds derived from medicinal herbs have been extensively studied and proposed as alternative treatments for several cancers. Investigators continually seek preparations from such plants that are efficacious without being unduly toxic. Curcumin is one such derivative and we selected it as the protagonist of this study. Curcumin, a yellow pigment derived from the rhizome of *Curcuma longa*, is one of the most-studied natural compounds for cancer treatment. It has several health-beneficial properties particularly anti-inflammatory, anti-infection and also anti-fibrosis activities (Pinlaor et al. 2010; Razavi et al. 2021). Curcumin is a promising agent for prevention and treatment of cancers in animal models including *O. viverrini*-associated CCA (Pinlaor et al. 2009; Prakobwong et al. 2011b), and clinical trials of curcumin have been introduced for many cancer types (Mansouri et al. 2020; Shehzad et al. 2010). It has been reported to be extremely safe in animals and humans, even at oral doses up to 8 g/day (Dei Cas and Ghidoni 2019). However, curcumin has several unfavorable properties, especially poor water solubility, low bioavailability and it is prone to degradation (Anand et al. 2007; Baker 2017; Liu et al. 2016), limiting its activity. Efforts have therefore been made to overcome these unfavorable properties (Mahran et al. 2017; Rafiee et al. 2019; Zhang et al. 2019).

One of the approaches is incorporation of curcumin into nanocarrier systems such as lipid-based nanocarriers, polymer-based nanocarriers, hydrogels, dendrimers and so on (Ipar et al. 2019; Rafiee et al. 2019; Zhang et al. 2019). Incorporation of curcumin into a mucoadhesive polymeric nanocarrier to deliver this payload into the gastrointestinal tract has been particularly promising (Suwannateep et al. 2011). Polymeric nano-curcumin has recently been improved by covering particles with xanthan and arabic gums—so-called curcumin-loaded nanocomplexes (CNCs) (Pinlaor et al. 2021). CNCs have very low toxicity for biliary epithelial cells and exhibit anti-CCA activity against CCA cell lines (Pinlaor et al. 2021). Similarly, CNCs have very low acute and chronic toxicity in animal models (Jantawong et al. 2021). However, attenuation of progression of CCA by CNCs in vivo has not yet been demonstrated.

The objective of this study was to assess the effect of a 5 month regimen of treatment with CNCs against CCA induced in a hamster model by *O. viverrini* infection. In this model, there is poor prognosis due to multi-site metastasis. Assessment of animal survival, number of tumors, histopathological changes, biochemical parameters, and the expression of inflammatory/oncogenic transcription factors were all investigated to assess the attenuation efficacy of CNCs on tumor development. This preclinical study should be a basis for translation to eventual clinical use.

Materials and methods

Chemicals and reagents

Curcumin (>98% purity w/w) was purchased from ACROS Organics (Geel, Belgium). ECL™ Prime Western blotting detection reagent and polyvinylidene difluoride (PVDF) membrane were purchased from GE Healthcare (Piscataway, NJ, USA). Rabbit anti-FOXM1 (C-20) was obtained from Santa Cruz (Dallas, Texas, USA). Horseradish peroxidase (HRP)-conjugated secondary antibody was purchased from Jackson ImmunoResearch (West Grove, PA, USA). Rabbit anti-β-actin, p65, RIPA buffer and bovine serum albumin were purchased from Cell Signaling Technology (Danvers, MA, USA). Rabbit anti-CK-19, anti-AFP, anti-HMGB1 and anti-PCNA were purchased from Abcam

(Cambridge, MA, USA). High glucose (4.5 g/L) Dulbecco's modified Eagle's medium (DMEM), fetal bovine serum (FBS), penicillin/streptomycin and 0.25% trypsin–EDTA were purchased from Gibco; Life Technologies (Grand Island, NY, USA). Siomycin A (SioA), a FOXM1 inhibitor, was purchased from Calbiochem (Billercia, CA, USA). Dehydroxylmethylepoxyquinomicin (DHMEQ), a specific inhibitor for NF-κB, was provided by Prof.Kazuo Umezawa, Aichi Medical University, Japan.

Preparation of CNCs

Curcumin-loaded nanocomplexes (CNCs, WellCap® Kaminn, encapsulation efficiency = 80%, loading capacity = 28%, particle size 400–1000 nm) and blank nanocomplexes (BNCs, WellCap® Capsule) powder were obtained from Welltech Biotechnology Co. Ltd. Bangkok, Thailand. CNCs were prepared according to a previously described (Pinlaor et al. 2021).

Animals

Male Syrian golden hamsters (*Mesocricetus auratus*) ($n = 160$), 4–6 weeks old, weight 80–100 g, were obtained from the Animal Unit at the Faculty of Medicine, Khon Kaen University, Khon Kaen, Thailand. Animals were randomly selected and kept in their cages for at least 5 days before the start of the experiment. All animals were maintained under clean conventional conditions at 23 °C (± 2 °C) with relative humidity 30–60% and 12 h light/dark cycle. The animals were provided ad libitum a commercial pellet diet (CP-SWT, Thailand) with unlimited supply drinking water. To avoid bacterial contamination, the stainless-steel cages were washed once a week with Sunlight detergent (Unilever, Thailand), decontaminated using the antimicrobial reagent Dettol (Dettol, Thailand) and sawdust was changed twice per week.

Isolation of *Opisthorchis viverrini* metacercariae

Opisthorchis viverrini metacercariae were isolated from naturally infected cyprinid fishes by pepsin digestion as described previously (Pinlaor et al. 2009). Briefly, fishes were digested in 0.25% pepsin–1.5% HCl (Wako Pure Chemical Industries, Osaka, Japan) in 0.85% NaCl solution and *O. viverrini* metacercariae were isolated and counted. Viable cysts were used to infect hamsters. Fifty *O. viverrini* metacercariae were given to each hamster by intragastric gavage. *N*-nitrosodimethylamine (NDMA) was given as 12.5 ppm in drinking water.

Experimental design

Preliminary study on CNCs dose optimization

We wished to determine the optimal dose rates of CNCs for the main study. This was done using two preliminary experiments. In the first, 60 hamsters were divided into three experimental groups: (1) normal control (Normal, $n = 20$); (2) *O. viverrini* (OV) infection plus NDMA without any curcumin treatment (ON, $n = 20$); (3) OV plus NDMA and treated with 178.57 mg/kg/bw of CNCs (equivalent to 50 mg cur/kg bw) daily for 5 months (ON + CNCs 50 mg) ($n = 20$). Hamsters in the relevant groups were infected with 50 *O. viverrini* metacercariae and 1 week later they were given NDMA together with CNCs.

Given the high mortality in the ON+CNCs 50 mg group, we then used a smaller-scale experiment with fewer animals. Ten hamsters were randomly divided into five groups: (1) normal control (normal, $n=2$); (2) *O. viverrini* (OV) infection plus NDMA without any curcumin treatment (ON, $n=2$); (groups 3–5), OV plus NDMA and treated with 35.71, 71.43 and 142.86 mg/kg/bw of CNCs (equivalent to 10, 20, and 40 mg cur/kg bw), respectively (ON+CNCs, $n=2$ each). Hamsters in the relevant groups were infected with 50 *O. viverrini* metacercariae and 1 week later they were given NDMA together with CNCs (thrice a week) for a subsequent 1 month.

Experimental animals used to determine the effect of CNCs on progression of CCA

Ninety hamsters were divided into five groups: (1) normal control (normal, $n=20$); (2) a combination of *O. viverrini* (OV) infection and NDMA without any treatment (ON, $n=30$); OV plus NDMA followed by administration of BNCs (3) (ON+BNCs, 71.43 mg/kg bw, $n=10$), or CNCs (4) 35.71 mg/kg (ON+CNCs, equivalent to 10 mg cur/kg bw, $n=15$) or (5) CNCs 71.43 mg/kg (ON+CNCs, equivalent to 20 mg cur/kg bw, $n=15$).

Commencing 1 week after infection with *O. viverrini* metacercariae, hamsters were given CNCs or BNCs thrice a week for 5 months. NDMA solution (12.5 ppm) was added to water, which animals were allowed to access ad libitum, for the first 2 months of the experiment. Body weights were recorded weekly. After the end of the experiment, all animals were starved for one day before being euthanized.

Sample collection

At the end of the study, hamsters were anesthetized and euthanized by isoflurane inhalation. Blood and liver tissue were collected. For the preliminary experiment to determine the optimal dose of CNCs, only biochemical parameters, liver-weight to body-weight ratio and histopathology were analyzed. Tumor volumes (TV) were measured using the formula $TV = (length \times width^2)/2$, where length represents the longest diameter of the tumor and width represents the smallest diameter of the tumor (Carlsson et al. 1983). Blood was collected by cardiac puncture and placed into clotted blood tubes and centrifuged at 3500 rpm at 4 °C for 10 min. Serum was separated and aliquoted and kept at − 20 °C until used for measurement of biochemical parameters. For histopathology and immunohistochemical tests, liver tissues were collected and fixed in 10% buffered formalin. For western blot analysis, liver samples were collected in liquid nitrogen as snap-frozen samples and kept at − 20 °C until used.

Biochemical measurement

Activities of liver function enzymes and levels of other biochemical parameters in serum of hamsters were measured using a Cobas 8000 Chemistry Autoanalyzer (Roche Diagnostics International Ltd., Scotland). The data were reported as means ± SD.

Histopathology

Liver tissues were fixed in 10% buffered formalin and paraffin-embedded sections were cut at 4 μm thickness and stained with hematoxylin and eosin (H&E) as well as with alcian blue/PAS for mucins. The grading approach for classifying inflammatory responses, both in terms of distribution and quantity, followed the International

Harmonization of Nomenclature and Diagnostic Criteria for Lesions in Rats and Mice (INHAND) (Thoolen et al. 2010). Cholangiofibrosis, cholangiofibroma and CCA lesions were assessed on all lobes of the liver. Cholangiofibrosis is a specific ductular reaction originating from initial oval cell hyperplasia in response to pronounced hepatic parenchyma necrosis (Narama et al. 2003; Thoolen et al. 2010). Chronic active inflammation grades were based on the degree of neutrophilic and mononuclear inflammatory cell infiltration, and of inflammatory cell exudates in bile duct lumens, portal interstitial tissue or adjacent liver parenchyma. Scores are presented separately for both perihilar bile duct and peripheral bile duct as follows: grade 0, no cholangitis: grade 1, marginal cholangitis: grade 2, slight cholangitis: grade 3, moderate cholangitis, grade 4, marked cholangitis and grade 5, severe cholangitis (Thoolen et al. 2010). Grading scores and pathology diagnosis were assigned in a double-blind manner by at least two independent researchers.

Immunohistochemistry and immunofluorescence

Liver sections (4 μm thickness) from all main experimental groups were subjected to immunohistochemistry and immunofluorescence. Rabbit anti-CK19 (1:100, ab15463, Abcam, UK), rabbit anti-AFP (1:500, GA500, Dako Omnis, USA), rabbit anti-PCNA (1:1000, ab2426, Abcam, UK) and rabbit anti-HMGB1 (1:350 ab79823, Abcam, UK) were used in 1% fetal bovine serum (FBS) overnight in a humidified chamber at 4 °C. After washing with phosphate-buffered saline (PBS) solution, slides were incubated with a 1:200 dilution of horseradish peroxidase (HRP)-labeled goat anti-rabbit IgG for 1 h at room temperature. The immunoreactivity signal was generated using diaminobenzidine substrate and the sections were counterstained with Mayer's hematoxylin and assessed using light microscopy. Ten fields (200 × magnification) of each slide were randomly selected and an image captured using a Nikon E600 microscope, Melville NY, USA. Grading of each image was done by three separate researchers. The percent positive area (blue stack) was quantified using ImageJ software (National Institutes of Health, Bethesda, MD, USA) (Bai et al. 2016).

   The formation of 8-NG in tissue sections was investigated by immunofluorescence as previously described (Pinlaor et al. 2009; Prakobwong et al. 2011b). Briefly, liver tissues were incubated with proteinase K 1:1000 for 3 min and followed in non-specific blocking with 5% bovine serum albumin. Then, tissue sections were incubated with rabbit anti-8-NG (1:50, Provided by Prof.Shosuke Kawanishi, Faculty of Health Science, Suzuka University of Medical Science, Suzuka, 510–0293, Japan) overnight at 4 °C. After washing, slides were incubated with Alexa 594-labeled goat anti-rabbit IgG (dilution 1:400) for 3 h at room temperature. Finally, the samples were mounted with VECTASHIELD® PLUS Antifade Mounting Medium with DAPI (Vector Laboratories, US). Stained tissues were investigated using a fluorescence microscope (Olympus BX63, Japan).

Western blot analysis

Twenty to 40 μg of protein extracted from each hamster liver was separated by sodium dodecyl sulfate polyacrylamide-gel electrophoresis (SDS-PAGE*)*, 7% separating gel, 5% stacking gel and then transferred to a polyvinylidene fluoride (PVDF) membrane. The membranes were probed with 1:1000 dilutions of primary antibodies for either rabbit

anti-NF-κB (cat. no. ab7970, Abcam, UK), rabbit anti-FOXM1 [C-20, obtained from Santa Cruz Biotechnology (Santa Cruz, CA, USA)] or mouse anti-β-actin (cat. no. ab 3280, Abcam, UK) at 4 °C overnight. After washing with 0.05% PBS-T, membranes were incubated with HRP-conjugated secondary antibody (1:3000) at room temperature for 1 h. Reactive bands were detected using chemiluminescence (ECL Plus, GE Healthcare). The intensity of reaction bands was quantified using the ImageJ open platform software, https://imagej.nih.gov/ij/plugins/ (NIH, Bethesda, MD).

Cell culture

The human cholangiocarcinoma cell line KKU-213B was obtained from the Japanese Collection of Research Bioresources (JCBR) Cell Bank, Osaka, Japan. The cells were cultured in high glucose (4.5 g/L) Dulbecco's modified Eagle's medium (DMEM) containing 10% heat-inactivated fetal bovine serum (FBS) and 1% of penicillin/streptomycin, and maintained at 5% CO_2 and 37 °C in a humidified incubator (Thermo Scientific, Waltham, MA). At 80% confluence, KKU-213B was trypsinized using 0.25% trypsin–EDTA and subjected to subsequent assays.

Cell viability assay of CNCs against CCA cell line

The MTT assay was performed to investigate the viability of CCA cells. Briefly, KKU-213B cells were seeded in 96-well culture plates (2×10^3 cells per well) and incubated overnight. The cells were then treated with either 0.5% DMSO as a vehicle control or various concentrations of CNCs (0–100 µg/ml) for 24 and 48 h. Thereafter, 10 µl of MTT solution (0.5 mg/ml) (Invitrogen; Thermo Fisher Scientific, USA) was added in each well and incubated at 37 °C for 4 h. Dimethyl sulfoxide (DMSO) (AppliChem Gmbh, Germany) was added to solubilize the formazan complex. The color intensities of samples were measured at 540 nm using a microplate reader (TECAN, Austria). The half maximal inhibitory concentration (IC_{50}) was analyzed using the dose–response inhibition mode of the GraphPad Prism® 8.0.1 software (GraphPad software, Inc., San Diego, CA, USA).

Clonogenic assay

KKU-213B cells were plated at a density of 7.5×10^4 cells/well in 6-well culture plates and allowed to attach overnight. Then, cells were treated with SioA (FOXM1 inhibitor), DHMEQ (NF-κB inhibitor) and CNCs 5 and 20 µg/ml. After 48 h of incubation, cells were trypsinized and plated onto a new 6-well culture plate at the density of 600 cells/well in fresh medium and kept without the drugs for 8 days. Thereafter, the colonies were fixed with absolute methanol and stained with 0.5% crystal violet in 1% acetic acid for 1 h. Plates were washed with water, left to dry out and photographed. Colonies were counted using Image-Pro Plus analysis software (Media Cybernetics, Inc.).

Cell cycle analysis using flow cytometry

KKU-213B (7.5×10^4 cells) was seeded into 6-well plates overnight. After that, cells were treated with SioA, DHMEQ and CNCs 5 and 20 µg/ml for 48 h. Then, cells were harvested, fixed with ice-cold 70% ethanol and kept at -80℃ overnight. The cells were stained with 500 µl of FxCycle PI/Rnase Staining Solution (Molecular Probes, Life

Jantawong *et al. Cancer Nanotechnology*   (2023) 14:5

Page 8 of 25

Technologies, USA) and incubated for 30 min at room temperature in the dark. DNA content of the cells was measured using flow cytometry (Becton Dickinson, FACSCanto II, BD Biosciences, San Jose, CA, USA). The percentages of cells in each phase were determined using FlowJo™ software.

Immunocytofluorescence staining

KKU-213B cells (7.5×10^4 cells per well) were plated in 6-well plates and treated with SioA (FOXM1 inhibitor), DHMEQ (NF-κB inhibitor) and CNCs for 48 h. The cells were trypsinized and plated on a cell culture slide (SPL life sciences, Korea) at a density of 2×10^4 cells per well. After the cells had adhered overnight, they were fixed with 4% paraformaldehyde, permeabilized with 0.2% Triton X-100 and blocked non-specific protein with 5% bovine serum albumin. The cells were then incubated with primary antibodies (anti-iNOS 1:500, Ab3523, Abcam and anti-Cdc25A, 1:500 from Santa Cruz Biotechnology, Inc., California, USA) at 4 °C overnight. Then, the cells were washed with PBS and incubated with secondary antibodies (Alexa Flour 488 and 568, 1:1000) for 2 h at room temperature. Excess unbound antibody solution was washed off with PBS, then nuclei were stained with Hoechst 33342 solution (1:7000, Molecular Probes, Life Technologies, USA). Finally, the samples were mounted with antifade mounting medium, visualized and photographed with fluorescence microscope (Nikon Corp, Japan).

Statistical analysis

Survival rate of hamsters was analyzed using Kaplan–Meier analysis. Graded scores of the stained tissue sections were compared using the non-parametric Mann–Whitney *U* test, using IBM SPSS statistics, version 23. The data are reported as means ± SD. To compare different experimental conditions, data were analyzed using analysis of variance (one-way ANOVA) along with post hoc tests. *P*-values of < 0.05 were considered to be statistically significant.

Results

Optimization for the effective dose and timing of curcumin content in CNCs

Our first preliminary study showed that an oral daily dose of CNCs at 50 mg cur/kg bw for 5 months led to a poor survival rate when compared with normal controls (Additional file 1: Fig. S1). We therefore determined the appropriate CNCs dose by treating the animals with a range of lower doses of CNCs thrice a week. All hamsters in this second initial trial survived when treated with CNCs (equivalent to 10, 20 and 40 mg cur/kg bw) thrice a week for 1 month, and some biochemical assays, including those for globulin, direct bilirubin and ALT, indicated decreased levels when compared with the ON group. In particular, levels of AST were significantly lower than in the ON group, indicating that CNCs can prevent liver injury. Notably, these biochemical parameters were significantly lower in the groups treated with CNCs 10 and 20 mg cur/kg bw thrice weekly than in those dosed at 40 mg cur/kg bw (Additional file 3: Table S1). The liver was brown without gross tumor lesions apparent at any dose rate. Reduction of inflammation was much greater after treatment with 10 and 20 mg cur/kg bw than with 40 mg cur/kg bw (Additional file 2: Fig. S2A). Body weight gain (Additional file 2: Fig. S2B), body weight before and after the experiment (Additional file 2: Fig. S2C) and liver-weight

to body-weight ratio (Additional file 2: Fig. S2D) did not differ significantly among all experimental groups due to small sample size ($n = 2$ per group). Thus, CNCs doses of 10 and 20 mg cur/kg bw, administered three times a week, were chosen for further experimental investigation.

CNCs increase survival of animals with CCA

After 5 months (159 days), 95% (19/20) of hamsters in the control group were still alive (Fig. 1). Survival rate of animals in the ON, ON + BNCs and ON + CNCs (both concentrations) groups were significantly lower than in the controls. In the ON group, the survival rate was 40% (12/30). Survival rates in groups given CNCs at dosages of curcumin equivalent to 10 and 20 mg cur/kg bw were 66.67% (10/15) and 53.33% (8/15), respectively, which were significantly higher than the ON group. In the ON + BNCs group, the survival rate was 40% (4/10), which was similar to that in the ON group (Fig. 1).

CNCs reduce macroscopic lesion appearance and improve body weight and liver-weight to body-weight ratio

Gross pathology of hamster livers is shown in Fig. 2A. The largest tumor mass with multiple white spots was seen in the ON and ON + BNCs groups, but fewer lesions were present in ON + CNCs 10 and 20 mg cur/kg bw.

Body weight gains were lower than normal controls in the ON group and in the two ON + CNCs groups, but higher in the BNC treatment group. The body weight gain in the ON group was significantly lower than in the BNCs group, as shown in Fig. 2B. Relative body weight had increased significantly in all experimental groups by the end of the experiment (Fig. 2C). In addition, liver-weight to body-weight ratios among ON, ON + BNCs and ON + CNCs (both concentrations) groups were all similar and were significantly higher than normal hamsters (Fig. 2D).
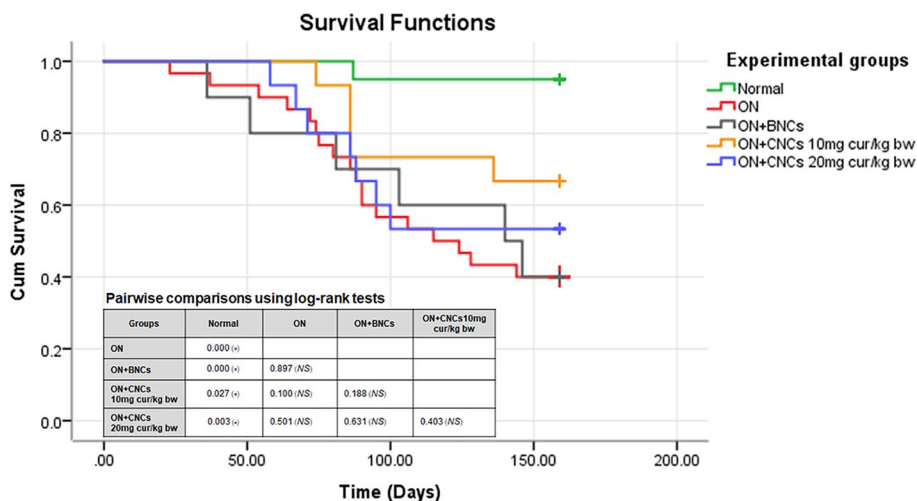

Fig. 1 Kaplan–Meier plots of survival rates in animals. Hamsters were divided into five groups; normal controls (green, $n = 20$), a combination of *Opisthorchis viverrini* infection and *N*-nitrosodimethylamine administration (ON, red, $n = 30$), ON followed by administration of CNCs containing 10 mg curcumin/kg bw (ON + CNCs 10 mg, orange, $n = 15$) and 20 mg curcumin/kg bw (ON + CNCs 20 mg, blue, $n = 15$), and blank nanocomplexes (ON + BNCs, gray, $n = 10$). CNCs and BNCs were administered thrice a week. Animals were maintained on these regimes for 5 months and survival was recorded daily
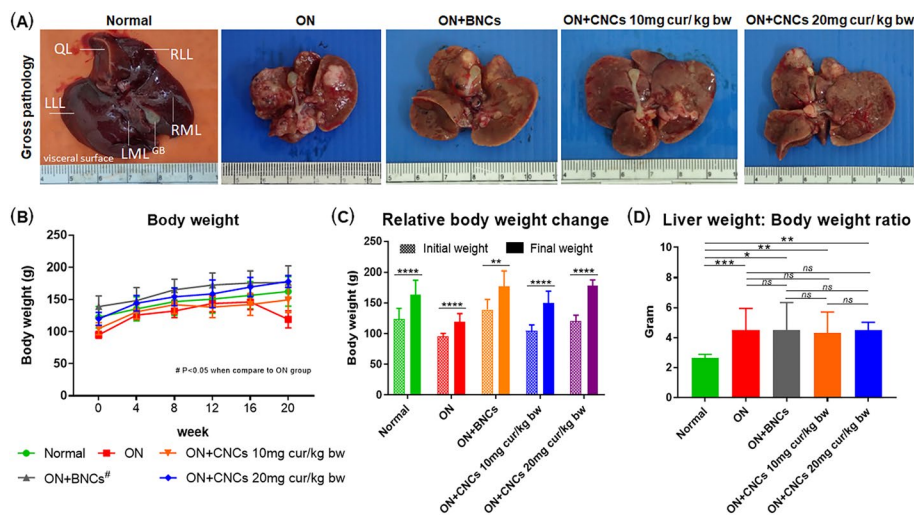
Fig. 2 Development of CCA in hamsters was induced by a combination of *Opisthorchis viverrini* (OV) infection and *N*-nitrosodimethylamine (NDMA) using treatment thrice a week for 5 months. **A** Representative gross appearance. **B** Body weight gain. **C** Relative body-weight change and **D** Liver weight to body weight (LW:BW) ratio in each experimental group at the end of 5 months. Experimental groups are identified in the legend for Fig. 1. *QL* quadrate lobe, *RLL* right lateral lobe, *LLL* left lateral lobe, *RML* right middle lobe, *LML* left middle lobe, *GB* gall bladder

Table 1 Changes in serum chemistry parameters after 5-month treatment with BNCs or CNCs thrice a week in hamsters in which CCA was induced by a combination of *Opisthorchis viverrini* infection and administration of a carcinogen

Parameters	Reference range	Unit	Experimental groups				
			Normal	**ON induced**			
				Untreated (ON)	**ON + BNCs**	**ON + CNCs 10 mg cur/ kg bw**	**ON + CNCs 20 mg cur/ kg bw**
			n = 19	*n* = 12	*n* = 4	*n* = 10	*n* = 8
Total protein	4.5–7.5	g/dL	6.04 ± 0.27	5.98 ± 0.43	5.55 ± 0.60	6.00 ± 0.27	6.08 ± 0.55
Albumin	2.3–4.3	g/dL	3.66 ± 0.20	3.11 ± 0.31*	2.70 ± 0.92*	3.31 ± 0.17@	3.10 ± 0.40*
Globulin	2.3–4.3	g/dL	2.37 ± 0.21	2.87 ± 0.33*	2.85 ± 0.40*	2.69 ± 0.25*	2.98 ± 0.27*
Total bilirubin	NA	mg/dL	0.03 ± 0.05	0.22 ± 0.16*	0.33 ± 0.39*	0.26 ± 0.21*	0.34 ± 0.32*
ALT	22–128	U/L	54.53 ± 19.23	272.64 ± 105.95*	288.75 ± 82.09*	261.13 ± 113.86*	270.43 ± 164.17*
AST	20–150	U/L	98.67 ± 51.90	126.83 ± 44.19	149.50 ± 61.11	149.29 ± 31.22	115.83 ± 36.45
Alkaline phosphatase	50–186	U/L	68.21 ± 30.85	100.17 ± 23.84*	76.50 ± 35.34	74.50 ± 14.13	83.13 ± 16.00

Data are mean ± SD and analyzed by one-way ANOVA

BNCs blank nanocomplexes, *CNCs* curcumin-loaded nanocomplexes, *ON* a combination of *Opisthorchis viverrini* infection and administration of *N*-nitrosodimethylamine, *mg cur/kg bw* mg curcumin/kg body weight. *NA* not available *P value < 0.05 compared to normal group

@ *P* value < 0.05 compared to ON + BNC group, n = number of killed animals at the end of experiment and used for biochemistry analysis. Data from animals dying before the end of the experiment were not analyzed

CNCs alter biochemical parameters associated with liver injury

Table 1 shows the effects on biochemical parameters after oral administration with CNCs thrice a week for 5 months in hamsters with ON-induced CCA. Although total

Table 2 Histopathological findings in hamster livers

Experimental groups		Percentage survival rate (mean ± SD)	Grading				CCA incidence	
			Chronic active inflammation score (mean ± SD)		Cholangiofibrosis (mean ± SD)	Cholangiofibroma (mean ± SD)	Percent of hamsters developing CCA (No. of hamsters)	Tumor volumes (mm^3) (mean ± SD)
			Perihilar bile duct	Peripheral bile duct				
Normal		95% (19/20)	0.00 ± 0.00	0.00 ± 0.00	0.00 ± 0.00	0.00 ± 0.00	0% (0/19)	0.00 ± 0.00
ON induced	Untreated	40% (12/30)	4.40 ± 0.84*	5.00 ± 0.00*	2.30 ± 2.06*	2.40 ± 2.37*	50% (6/12)	47.35 ± 78.71*
	ON + BNCs	40% (4/10)	3.25 ± 0.50$^{*,\#}$	4.50 ± 0.58*	2.25 ± 0.50*	3.50 ± 2.38*	50% (2/4)	38.97 ± 23.95*
	ON + CNCs 10 mg cur/kg bw	66.67% (10/15)	2.70 ± 0.67$^{*,\#}$	3.90 ± 0.88$^{*,\#}$	2.70 ± 1.83*	1.10 ± 1.85	30% (3/10)	22.36 ± 12.03*
	ON + CNCs 20 mg cur/kg bw	53.33% (8/15)	2.63 ± 0.92$^{*,\#}$	4.00 ± 0.93$^{*,\#}$	2.88 ± 1.13*	2.50 ± 0.93*	75% (6/8)	33.43 ± 39.98*

Data are mean ± SD

BNCs blank nanocomplexes, *CNCs* Curcumin-loaded nanocomplexes, *ON* a combination of *Opisthorchis viverrini* infection and *N*-nitrosodimethylamine

* *P* value < 0.05 compared to normal controls when analyzed by one-way ANOVA

$^\#$ *P* value < 0.05 compared to ON untreated group when analyzed by one-way ANOVA
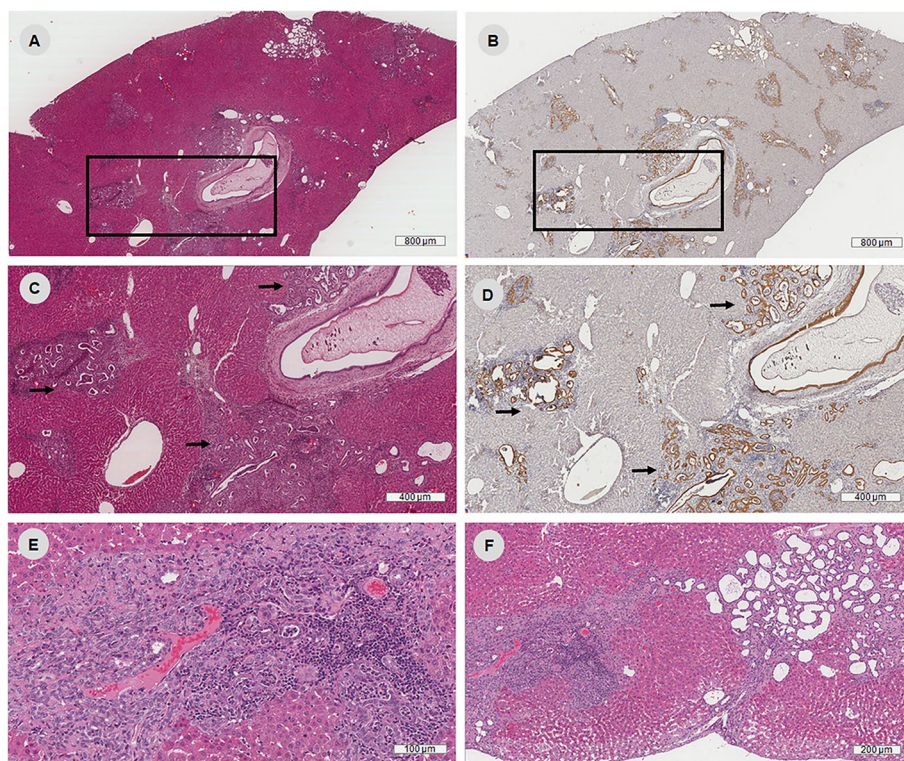
Fig. 3 Micrographs of chronic active cholangitis in hamster livers with obstructive cholestasis from the group infected with *Opisthorchis viverrini* and receiving NDMA, at 5 months. **A**, **B** overview of generalized cholangitis lesions in chronic obstructive cholestasis in opisthorchiasis, **A** H&E stain and **B** stained for cytokeratin 19, inset boxes indicate perihilar areas. **C**, **D** Chronic active cholangitis (black arrows) at the perihilar area, **C** H&E stain and **D** cytokeratin 19. **E** Chronic active cholangitis of peripheral bile ducts at the subcapsular area, showing inflammatory exudates in bile duct lumens and mixed inflammatory cell infiltration in periductal and interstitial tissue. **F** peripheral bile ducts at the subcapsular area, **F**, **left** reveals chronic cholangitis and **F**, **right** reveals healed cholangitis foci

protein did not much change in all experimental conditions, levels of albumin had significantly decreased and levels of globulin, total bilirubin and ALT had significantly increased in ON, ON+BNCs and ON+CNCs (both concentrations) groups relative to normal controls. The greater serum AST levels in ON, ON+BNCs and ON+CNCs (both concentrations) groups were all similar and did not significantly differ from levels in the normal control group. Serum alkaline phosphatase level was significantly higher than in controls in the ON group, but its level was reduced after CNCs treatment (10 and 20 mg cur/kg bw). Unexpectedly, the level of alkaline phosphatase in the BNCs treatment group was comparable to that in the CNCs treatment groups.

CNCs delay tumor development and attenuate the severity of liver histopathological changes in livers

Fifty percent of hamsters (6/12) developed CCA in the ON group and 50% (2/4) in the ON+BNCs group. In the ON+CNCs (10 mg cur/kg bw) group, 30% of hamsters (3/10) developed CCA. Unexpectedly, 75% (6/8) hamsters in the ON+CNCs (20 mg/kg bw) group developed CCA, suggesting that adverse effects may have resulted from
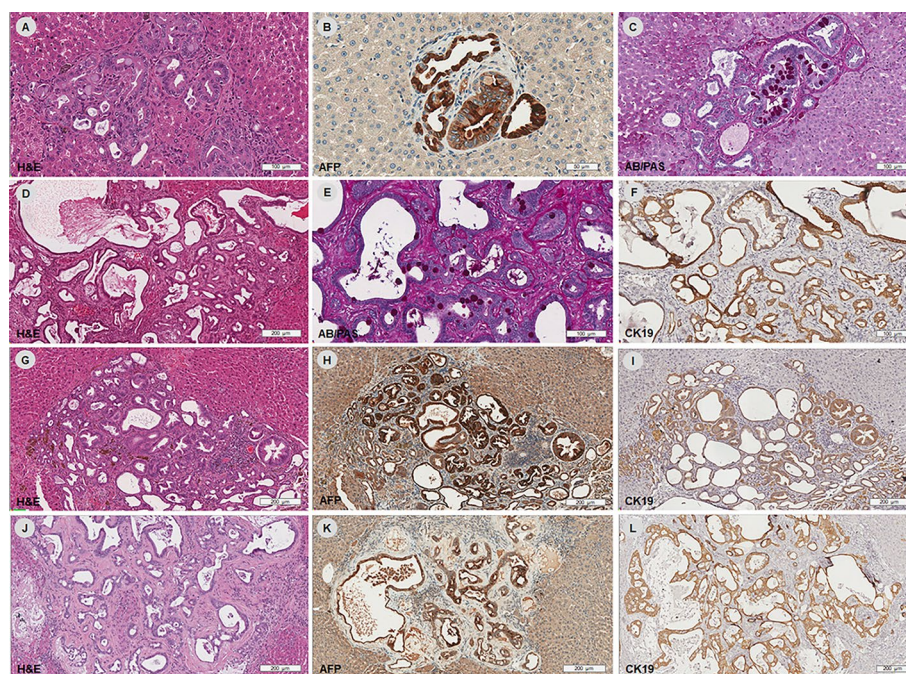
Fig. 4 Representative micrographs of xenobiotic-induced cholangiofibrosis and cholangiofibroma in hamster livers with *Opisthorchis viverrini* infection and receiving NDMA, after 5 months. **A**–**C** Early development of cholangiofibrosis, initially associated with oval cell proliferation and bile duct hyperplasia. **A** A lesion showing portal proliferation of bile ductules, lined by a single layer of cuboidal or columnar epithelium along with mucin-containing cells. **B** Ductular reaction cells are positive for AFP: a marker for bipotential oval cells. **C** AB/PAS: acid mucin was present in goblet cells (intestinal metaplasia). **D**–**F** Cholangiofibrosis consists of dilated to cystic bile ducts filled with mucus, cellular debris and surrounded by inflammatory cell infiltrates and connective tissue. **E** AB/PAS. **F** CK 19 was present in both biliary gland and glands with intestinal metaplasia. **G**–**I** Cholangiofibrosis, progressing lesion. **G** There is aggregation of the adjacent portal lesions, as well as ductal proliferation and cystic dilatation of metaplastic glands, peribiliary fibrosis and a mixed inflammatory cell infiltrate. **H**–**I** The lesion is positive for both AFP and CK19, indicating oval cell proliferation and developed in the line of cholangiocytes. **J**–**L** Cholangiofibroma. **J** Cholangiofibroma, expanding nodular formation of glandular and stroma components of cholangiofibrosis. **K**–**L** The lesion is positive for both AFP and CK19, similar to cholangiofibrosis

an overdose of curcumin. Tumor mass in hamster liver was measured and presented as tumor volumes (mm^3). Hamsters in the ON+BNCs group and the ON+CNCs (both concentrations) groups had lower tumor volumes than the ON group. This was especially marked in the ON+CNCs (10 mg cur/kg bw) group (Table 2).

The existence of CCA was also confirmed by H&E staining. In agreement with gross pathology, the ON group had the highest number of hamsters with cancer. Recurrent ascending cholangitis is common in chronic cholestasis found in hamsters infected with *O. viverrini*. A combination of acute and chronic inflammatory cells in bile ducts, periductal tissue and adjacent liver tissue was considered as chronic active inflammation (Thoolen et al. 2010). Figure 3 demonstrates chronic cholestasis due to chronic *O. viverrini* infection with chronic active inflammation and healing cholangitis, leading to occasional cholangiofibrosis. Histopathological changes in all experimental groups are summarized in Table 2. Cholangiofibrosis appears as minute grayish granules in the parenchyma. The lesion consists of hyperplastic bile ductules, intestinal metaplasia foci and fibrotic stroma (Fig. 4). Cholangiofibroma
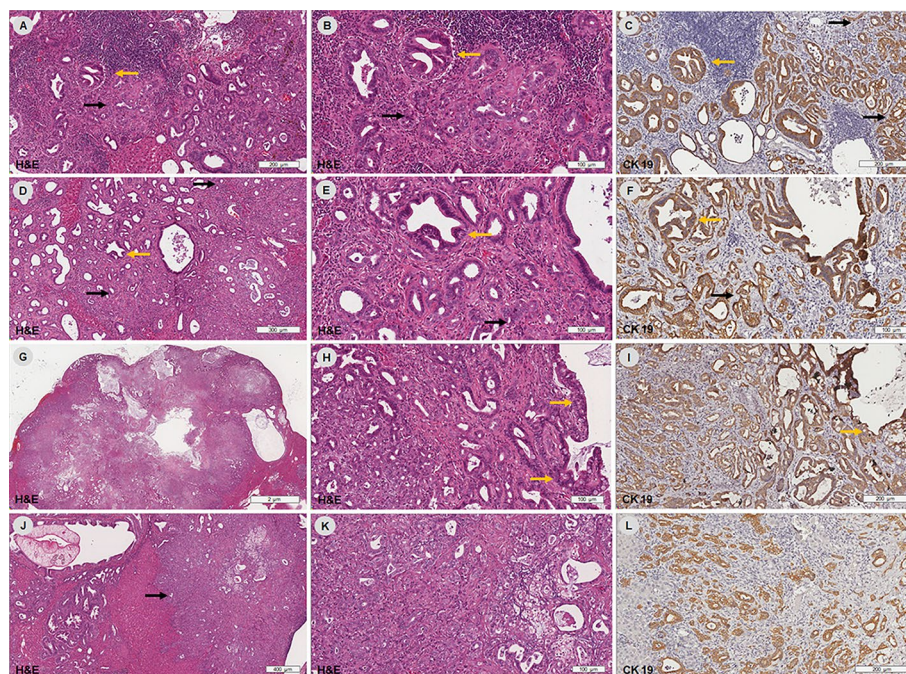
Fig. 5 Representative micrographs of cholangiocarcinoma (CCA) and its precursor lesions in H&E-stained sections. A primary lesion from the bile duct is indicated by CK19 staining, in hamster livers infected with *Opisthorchis viverrini* and receiving NDMA, at 5 months. **A**–**C** Malignant transformation of cholangiofibrosis; **D**–**F** malignant transformation of cholangiofibroma; CCA (black arrows). Note abnormal overlapping and piling up of cells and gland formation at a metaplastic duct (yellow arrows), with proliferation of atypical ductules in the hepatic parenchyma (black arrows). **G**–**I** CCA, a well-differentiated adenocarcinoma producing mucin; malignant transformation from a dilated metaplastic duct (yellow arrows), is noted. **J**–**L** CCA (black arrows), a moderately differentiated adenocarcinoma with mild production of mucin, malignant transformation foci are obscured

is an expanded nodule-forming cholangiofibrosis that appears as gray nodular or multinodular lesions with distinct borders and may compress adjacent liver tissue (Fig. 4). CCA shows as a grayish-white focal liver mass or cluster of nodules or plaque. It is an adenocarcinoma, composed of glands, solid sheets, trabeculae or closely packed ductules, with or without production of mucin (Fig. 5).

In the ON group, greater active inflammation, cholangiofibroma and tumor mass were clearly observed. The ON + BNCs group showed similar histological findings to the ON group. In contrast, these histopathological changes were less pronounced in the CNCs treatment group at 10 mg cur/kg bw, but this group exhibited increased cholangiofibrosis. Notably, hamsters treated with CNCs at 20 mg cur/kg bw exhibited more cholangiofibroma and higher tumor mass than did the hamsters treated with 10 mg cur/kg bw.

CNCs attenuate the progression of cholangiocarcinoma in hamsters

It is known that *N*-nitrosodimethylamine treatment combined with liver fluke infection causes both hepatocellular carcinoma and cholangiocarcinoma (Mitacek et al. 1999; Thamavit et al. 1994). We therefore confirmed that CCA was present by detecting the
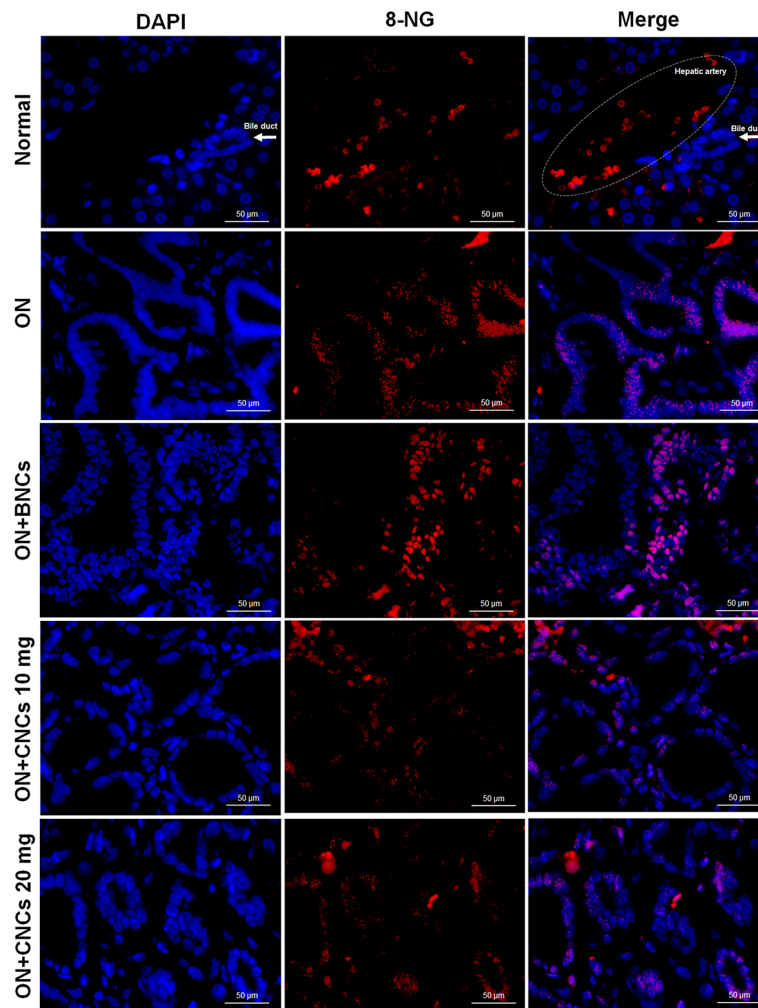
Fig. 6 Representative images of 8-nitroguanine (8-NG) formation in hamster liver tissues visualized by immunohistofluorescence staining. Rabbit anti-8-NG antibody and DAPI were used for staining nuclei. Formation of 8-NG (red) and DAPI (blue) in nuclei of bile duct epithelial cells and inflammatory cells is very evident in ON and ON + BNCs groups, but less so in ON + CNCs 10 mg and ON + CNCs 20 mg groups. Scale bar is 50 μm

expression of the bile duct marker, cytokeratin 19 (CK 19). Expression of CK19 was observed in all tumor lesions. PCNA, proliferation cell nuclear antigen, was used to investigate cell proliferation index and AFP was used to confirm pre-neoplastic lesions, as shown in brown color in cholangiofibrosis, but not in CCA. Periodic acid–Schiff (PAS) stain was used to confirm mucin in cholangiofibrosis (Fig. 4). PCNA expression was significantly greater in ON and BNCs treatment groups compared to normal controls. Its expression and distribution was significantly lower in both CNCs treatment groups, and especially in the 10 mg cur/kg bw group.

It is well known that chronic inflammation-mediated DNA damage is a key molecular mechanism of CCA genesis in OV-associated CCA (Pinlaor et al. 2005). We therefore investigated the expression of 8-nitroguanine, a DNA damage marker (Fig. 6). Immunofluorescence assay showed that 8-nitroguanine expression was increased in
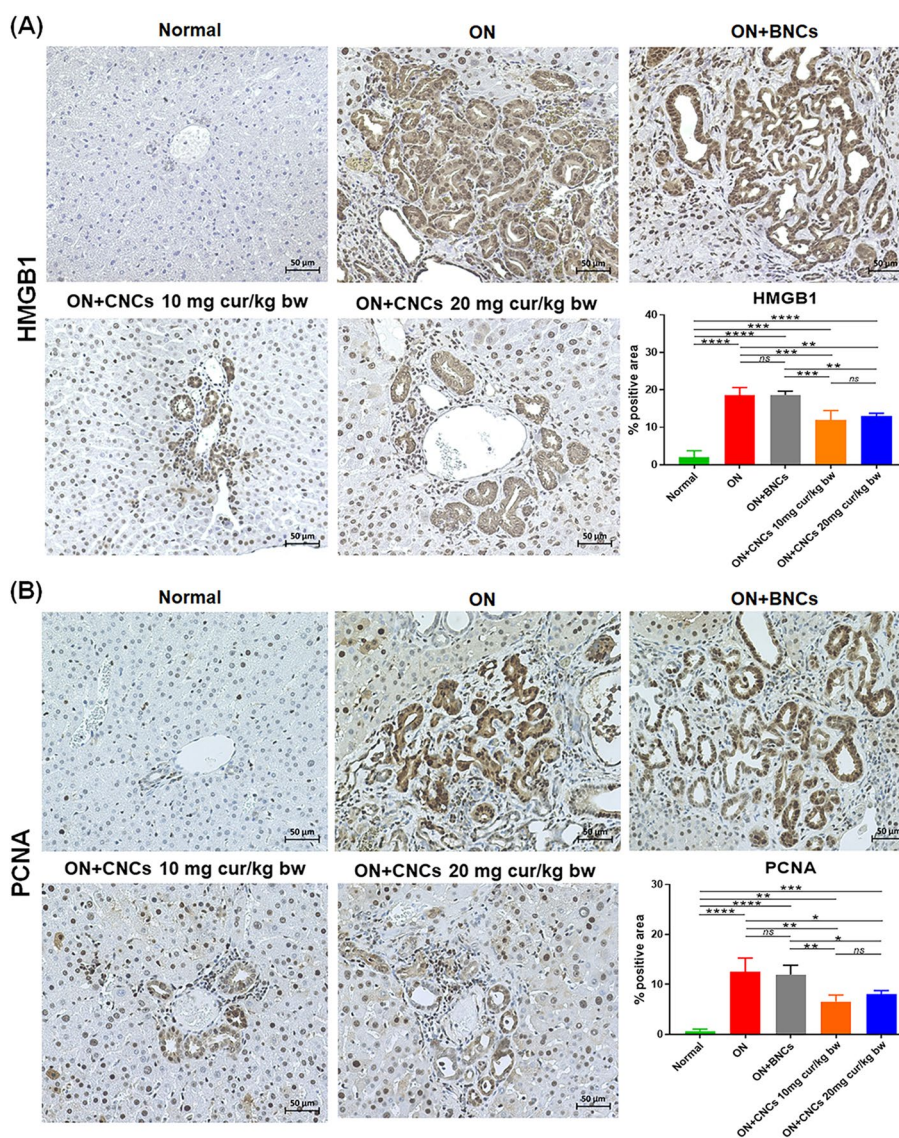
Fig. 7 Representative images of liver sections using immunohistochemical staining. **A** HMGB1 and **B** PCNA expression in liver tissues of hamsters from all experimental groups and grading score in liver tissue

the ON and ON + BNCs groups compared to normal controls. But that this expression was reduced by CNCs treatment at both dose rates of 10 and 20 mg cur/kg bw. An expression of high mobility group box-1 (HMGB1), an inflammatory marker associated with carcinogenesis, which is a potential therapeutic target for cancers (Vijaya-kumar et al. 2019). HMGB1 expression was mainly observed in the nucleus of bile duct epithelial cells and was highest in the ON and ON + BNCs groups. In contrast, HMGB1 expression was significantly lower in the CNCs treatment groups (both 10 and 20 mg cur/kg bw) compared to the ON group in Fig. 7. Expression levels of CK-19 and AFP also supported these findings.
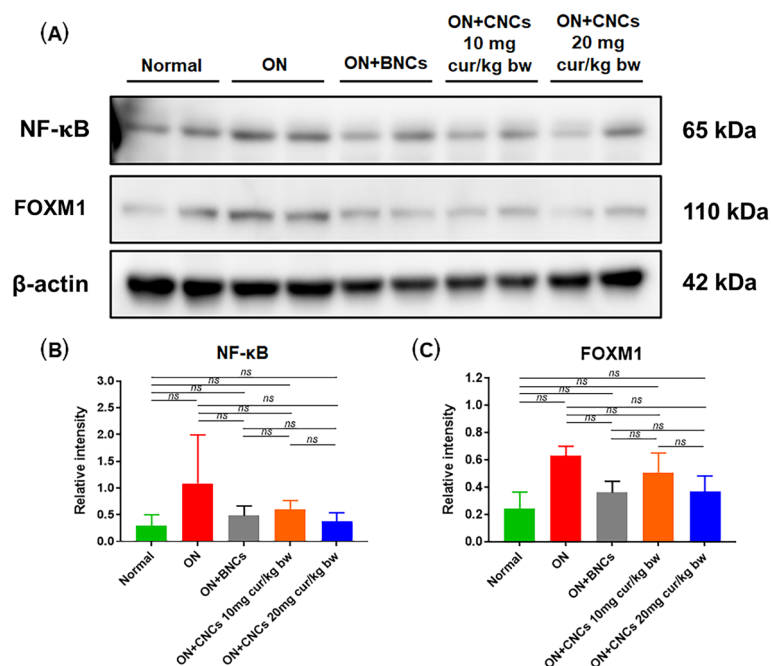
Fig. 8 Effect of CNCs on expression of transcription factors NF-κB and FOXM1 in hamster livers. **A** NF-κB and FOXM1 protein expression was measured by western blot. **B**, **C** Relative intensity of protein bands shown as a graph. All pairwise statistical comparisons were non-significant. Data are derived from duplicate independent experiments and presented with mean ± SD

CNCs suppress the expression of oncogenic transcription factors involved in cholangiogenesis

The effect of CNCs on the expression of oncogenic transcription factor NF-κB (65 kDa) and FOXM1 (110 kDa) is shown in Fig. 8. Western blot analysis showed that expression of both was greater in the ON group compared to normal controls, but was lower in groups treated with CNCs at both 10 and 20 mg cur/kg bw.

CNCs treatment inhibit proliferation of the CCA cell line

The effect of CNCs on growth of CCA cells was assessed. The MTT assay revealed that administration of CNCs decreased cell proliferation of KKU-213B cells in a dose- and time-dependent manner with IC_{50} values of 24.19 µg/ml for 24 h and 9.33 µg/ml for 48 h (Fig. 9A). The clonogenic assay was performed to determine replicative ability of the cells to form a colony. The results showed that CNCs significantly inhibited KKU-213B colony formation in a dose-dependent manner. Dehydroxylmethylepoxyquinomicin (DHMEQ) and Siomycin A (SioA) are a NF-κB inhibitor and a FOXM1 inhibitor, respectively, and were used to confirm the oncogenic signaling pathways. The result showed that CNCs 5 µg/ml, DHMEQ, SioA and DHMEQ + SioA all significantly inhibited the formation of colonies by KKU-213B cells relative to vehicle controls (Fig. 9B, C). Treatment with DHMEQ + CNCs 5 µg/ml reduced ability to form colonies more than did either of these alone. These results indicated that CNCs can inhibit the proliferation of CCA cells through oncogenic signaling pathways associated with NF-κB and FOXM1.
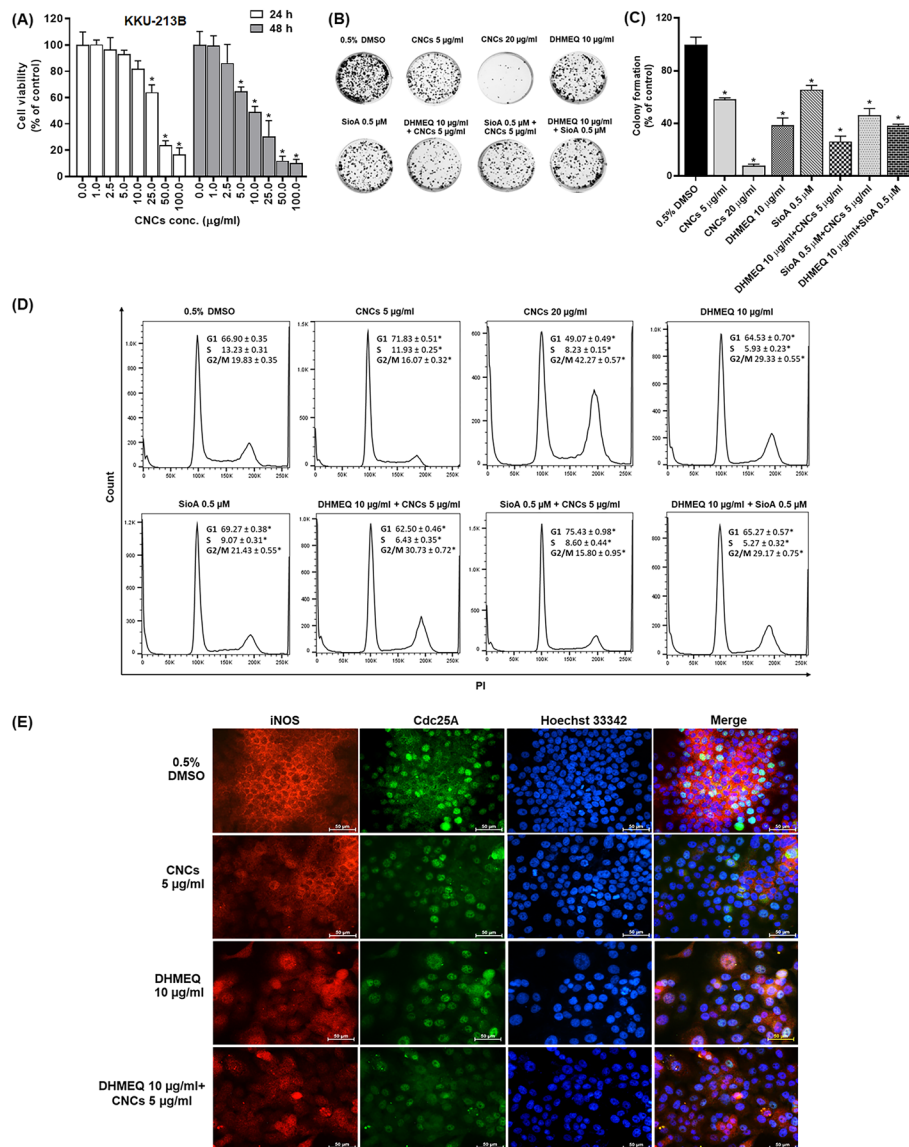
Fig. 9 Effects of CNCs on cell viability, cell division cycle. **A** Cell viability was assessed using the MTT assay. **B** Representative images from the colony-formation assay of KKU-213B cells under each designated treatment. **C** Percentage of colony formation assay was showed as group and compare with 0.5% DMSO control. **D** Representative image of cell cycle analysis detected using a flow cytometer. **E** Representative images of KKU-213B cells by immunocytofluorescence staining using iNOS, Cdc25A and Hoechst 33342. Scale bar is 50 µm. Data are mean ± SD from three independent experiments. *****P value < 0.05 versus vehicle control

CNCs induce KKU-213B cell cycle arrest

Cell division cycle analysis was performed to investigate the antiproliferation property of CNCs against KKU-213B CCA cells using flow cytometry. The result showed that CNCs significantly arrested cell-cycle progression at the G2/M phase in a dose-dependent manner as shown in Fig. 9D. These findings indicated that CNCs could inhibit the proliferation ability of CCA cells by interference with the cell division cycles.
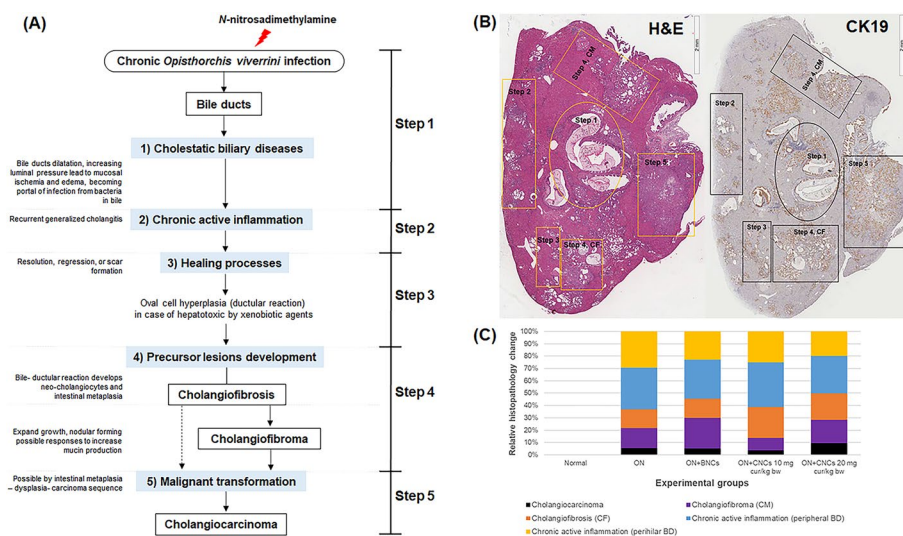
Fig. 10 Summary of attenuation effects of curcumin-loaded nanocomplexes (CNCs) in hamsters with cholangiocarcinoma induced by *Opisthorchis viverrini* (OV) infection and *N*-nitrosadimethylamine (NDMA) treatment after 5 months. **A** Hypothetical pathway of cholangiocarcinogenesis induction by combination of OV plus NDMA in hamsters. **B** Areas mapped to demonstrate pathological steps 1–5 in **A**, in a representative hamster liver. *CF* cholangiofibrosis, *CM* cholangiofibroma. **C** Comparison of relative histopathology observed in each experimental group

CNCs suppress the expression of iNOS and Cdc25A

To verify the involvement of NF-κB and FOXM1 in a CNCs-mediated tumor-suppression signaling pathway downstream of these oncogenic transcription factors, iNOS and Cdc25A, were investigated using immunocytofluorescence assays as shown in Fig. 9E. The result demonstrated that iNOS and Cdc25A expression was increased in the vehicle (0.5% DMSO) control group, but reduced by treatment with CNCs and DHMEQ + CNCs.

Discussion

In this study, we used an improved version of curcumin-loaded nanocomplexes (CNCs), known to be safe in mouse and hamster models (Jantawong et al. 2021) and with low cytotoxicity to normal fibroblast and cholangiocarcinoma cell lines (Pinlaor et al. 2021). These CNCs were tested for their ability to retard CCA development in hamsters. Relative to controls, oral administration of CNCs with curcumin equivalent to 10 and 20 mg/kg bw thrice a week for 5 months increased survival rate of animals, reduced inflammation, reduced percentage of hamsters with CCA, reduced serum alkaline phosphatase levels and improved the histopathological picture. This was especially the case for treatment with CNCs at 10 mg cur/kg bw. These effects may be exerted via suppression of NF-κB and FOXM1-mediated pathway. The consequence of histopathological changes by which CNCs suppress CCA induced by a combination of *O. viverrini* infection and *N*-nitrosodimethylamine treatment is summarized in Fig. 10.

Previous study demonstrated that native curcumin inhibits cholangiocarcinogenesis in our hamster/CCA model (Prakobwong et al. 2011b). CNCs exhibit anti-periductal fibrosis effects and could prevent bile canalicular abnormalities in *O.*

viverrini-infected hamsters (Charoensuk et al. 2016). To gain better control of the delivery of curcumin, CNCs were further enhanced by using a solid-dispersion method with gums. Gum-based nanocarriers served as important containers for the protection and delivery of some active compounds (Taheri and Jafari 2019). Importantly, these polysaccharides cannot be digested/degraded in strong acid condition such as in the stomach and small intestine, but are degraded in the colon by colonic bacteria (Salyers et al. 1977). Therefore, use of arabic and xanthan gums for curcumin delivery could prevent curcumin release and degradation in the stomach and small intestine, but ensures release in the colon instead (Ribeiro et al. 2016; Srikaeo et al. 2018; Taheri and Jafari 2019).

Many cancers, including *O. viverrini*-associated CCA, arise from infection through chronic irritation and inflammation (Kawanishi et al. 2006; Yongvanit et al. 2012). These in turn can lead to cholangiofibrosis, nodular cholangiofibrosis or cholangiofibroma and contribute to CCA development (Bannasch 2019; Chen et al. 2019; Thoolen et al. 2010). The glandular epithelium of both cholangiofibrosis and cholangiofibroma are typically lined with a simple layer of cuboidal or columnar cells. CK19 is usually expressed in ductal epithelium such as bile duct epithelium, pancreas and is also found in primitive hepatic progenitor cells. However, CK19 expression is not present in mature hepatocytes. This is why CK19 is a useful marker of cells of bile duct epithelial origin in liver tissue (Leelawat et al. 2012; Zhuo et al. 2020). In hamsters and rats, cholangiofibrosis and cholangiofibroma have been considered as precursor lesions of CCA (Bannasch 2019). Hamsters in the ON and ON + BNCs groups after 5 months usually exhibited chronic inflammation, lead to cholangiofibroma, developing in some cases into solid mass lesions of CCA. In contrast, hamsters treated with CNCs of either concentration had lower chronic active inflammation scores both for the perihilar bile duct and the peripheral bile duct, suggesting the anti-inflammation potential of curcumin (Razavi et al. 2021). In particular, hamsters given CNCs at the dose rate of 10 mg cur/kg bw showed increased cholangiofibrosis, but a decrease of cholangiofibroma and CCA, while the opposite was apparent in the ON and ON + BNCs groups. Hamsters given CNCs at 10 mg cur/kg bw were less likely to have CCA after 5 months: however, they still displayed cholangiofibrosis, a pre-neoplastic lesion. This implies that CNCs have the potential to delay CCA development by inhibiting chronic inflammatory processes at an initial step.

Adverse effects appear to have occurred in the group given the higher-dose treatment (ON + CNCs 20 mg cur/kg bw). This may be due to an overdose of this substance. Curcumin exerts pro-oxidant activity (Aggeli et al. 2013) and promotes gall bladder contraction (Rasyid et al. 2002) to release bile, as well as having an influence on bile flow (Wang et al. 2016) despite obstructions where adult *O. viverrini* occur, leading to increased bile duct proliferation. This suggests that dosage of CNCs should be considered carefully in diseases associated with biliary obstruction. The beneficial effect of a low-dose CNC treatment is in general agreement with a previous study in which a high dose of turmeric extract reduced inflammation (Boonjaraspinyo et al. 2009), and an appropriate curcumin dose reduced oxidative and

nitrative DNA damage (Pinlaor et al. 2009), periductal fibrosis (Pinlaor et al. 2010) and prevented alteration of bile canaliculi in hamsters with opisthorchiasis.

CNCs may retard CCA progression via the antiproliferation effect of curcumin on CCA cells (Prakobwong et al. 2011a) and the suppression of inflammation-mediated molecular and DNA-damage events associated with multistep carcinogenesis (Prakobwong et al. 2011b). Here, we found that CNC treatment reduced expression of NF-κB, the activator of transcription factors involved in inflammation-related carcinogenesis, and inhibited the expression of NF-κB-regulated gene products, including iNOS. Suppression of iNOS by CNCs reduces NO production leading to reduction in nitrative DNA damage, as indicated by reduced formation of 8-NG, a nitrative DNA-damage marker. Likewise, CNCs reduced HMGB1, a chromatin protein which stimulates production of NF-κB. By these means, CNCs attenuate inflammation. CNCs have an antiproliferation effect on KKU-213B CCA cells by disturbing the cell division process in the G2/M phase. Administration of CNCs led to reduced expression of Cdc25A, a cell cycle-associated protein controlling cell-cycle progression. CNCs also reduced expression of markers of cell proliferation including PCNA and FOXM1, which act downstream of NF-κB and transcriptional regulators in cell cycles. Upregulation of NF-κB (Dolcet et al. 2005), FOXM1 (Wierstra 2013), iNOS (Pinlaor et al. 2005) and HMGB1 (Vijayakumar et al. 2019) is involved in tumorigenesis of different cancer types, influencing processes ranging from development to drug resistance. For this reason, these molecules have been targeted for cancer therapy. Suppression by curcumin of NF-κB (Prakobwong et al. 2011a, 2011b), FOXM1 (Zhang et al. 2014), PCNA (Prakobwong et al. 2011b) and HMGB1 (Wang et al. 2012) that we noted was similar to many previous reports. Suppression of CCA development by curcumin might also be through targeting multiple proteins involved in CCA genesis (Khoontawad et al. 2018).

In addition to suppression of CCA development, CNC treatment could prevent liver damage, as evidenced by the decreased serum activity of ALT and AST and reduction of HMGB1 expression. Inhibition of the translocation and extracellular release of HMGB1 alleviates liver damage and fibrotic lesions (Bai et al. 2016). However, the specific mechanisms involved require further study.

Conclusion

We further evaluated the effect of CNCs on opisthorchiasis-associated CCA in hamsters. CNCs, solid dispersion of curcumin-loaded nanoparticles, exhibit greater efficacy to delay CCA development than does straight curcumin. Treatment with CNCs increased survival in animals, reduced tumor development, reduced bile duct injury and suppressed expression of NF-κB, FOXM1 and HMGB1. Based on our experiments, we suggest that CNCs at 10 mg cur/kg bw thrice a week is a promising dose rate for alleviation of CCA development in patients. CNCs, 35.71 mg/kg bw (equivalent to 10 mg cur/kg bw), as an effective dose to suppress CCA development, could be converted to a dose for clinical trials in patients at 28.95 mg/kg bw (an individual weighing 60 kg, dividing the human equivalent dose by tenfold safety factor) of CNCs.

Abbreviations

CCA	Cholangiocarcinoma
OV	*Opisthorchis viverrini*
CNCs	Curcumin-loaded nanocomplexes
BNCs	Blank nanocomplexes
cur	Curcumin
CK19	Cytokeratin 19
AFP	Alpha fetoprotein
PCNA	Proliferating cell nuclear antigen
HMGB1	High mobility group box 1
NF-κB	Nuclear factor kappa B
FOXM1	Forkhead box M1
8-NG	8-Nitroguanine
DHMEQ	Dehydroxylmethylepoxyquinomicin
SioA	Siomycin A
iNOS	Inducible nitric oxide synthase
Cdc25A	Cell division cycle 25A

Supplementary Information

The online version contains supplementary material available at https://doi.org/10.1186/s12645-023-00155-0.

Additional file 1: Fig S1. Kaplan–Meier plot of survival rates in hamsters fed CNCs 50 mg cur/kg bw daily for 5 months. Hamsters were divided into 3 groups; Normal controls (green, $n=20$), a combination of *Opisthorchis viverrini* infection and *N*-nitrosodimethylamine administration (ON, red, $n=20$), and ON followed by administration of CNCs containing 50 mg cur/kg bw (ON+CNCs 50 mg cur/kg bw, purple, $n=20$). Hamsters in the last group were given CNCs daily for 5 months and survival was recorded daily.

Additional file 2: Fig S2. Optimization of curcumin content in CNCs assessed using treatment thrice a week for 1 month. (A) Gross appearance and histopathological features of hamster livers. (B) Body weight gain. (C) Relative body weight change and (D) Liver weight to body weight ratio. Ten hamsters were divided into five groups; normal group, a group given a combination of *Opisthorchis viverrini* infection and *N*-nitrosodimethylamine (ON), and groups given ON followed by administration with CNCs of 10, 20 or 40 mg cur/kg body weight thrice a week for 1 month.

Additional file 3: Table S1. Optimization of curcumin content in CNCs on serum chemistry parameters after 1 month treatment for thrice a week in hamsters.

Availability of data and materials

Not applicable.

Declarations

Ethics approval and consent to participate

This study protocol was reviewed and approved by the Animal Ethics Committee of Khon Kaen University (ACUC-KKU-59/2559), based on the ethical guidelines for Animal Experimentation of the National Research Council of Thailand.

Consent for publication

Not applicable.

Competing interests

Welltech Biotechnology Co., Ltd, Thailand, the producer and supplier of CNCs and BNCs, had no part in the planning and conducting the experimental design in this project. The authors declare that they have no competing of interests.

References

Aggeli IK, Koustas E, Gaitanaki C, Beis I (2013) Curcumin acts as a pro-oxidant inducing apoptosis via JNKs in the isolated perfused rana ridibunda heart. J Exp Zool A Ecol Genet Physiol 319(6):328–339

Anand P, Kunnumakkara AB, Newman RA, Aggarwal BB (2007) Bioavailability of curcumin: problems and promises. Mol Pharm 4(6):807–818

Bai L, Kong M, Zheng Q, Zhang X, Liu X, Zu K et al (2016) Inhibition of the translocation and extracellular release of high-mobility group box 1 alleviates liver damage in fibrotic mice in response to D-galactosamine/lipopolysaccharide challenge. Mol Med Rep 13(5):3835–3841

Baker M (2017) Deceptive curcumin offers cautionary tale for chemists. Nature 541(7636):144–145

Banales JM, Marin JJG, Lamarca A, Rodrigues PM, Khan SA, Roberts LR et al (2020) Cholangiocarcinoma 2020: the next horizon in mechanisms and management. Nat Rev Gastroenterol Hepatol 17(9):557–588

Bannasch P (2019) Letter to the editor regarding "cholangiofibrosis and related cholangiocellular neoplasms in rodents." Toxicol Pathol 47(7):896–898

Boonjaraspinyo S, Boonmars T, Aromdee C, Srisawangwong T, Kaewsamut B, Pinlaor S et al (2009) Turmeric reduces inflammatory cells in hamster opisthorchiasis. Parasitol Res 105(5):1459–1463

Carlsson G, Gullberg B, Hafstrom L (1983) Estimation of liver tumor volume using different formulas—an experimental study in rats. J Cancer Res Clin Oncol 105(1):20–23

Charoensuk L, Pinlaor P, Wanichwecharungruang S, Intuyod K, Vaeteewoottacharn K, Chaidee A et al (2016) Nanoencapsulated curcumin and praziquantel treatment reduces periductal fibrosis and attenuates bile canalicular abnormalities in *Opisthorchis viverrini*-infected hamsters. Nanomedicine 12(1):21–32

Chen T, Chen K, Qiu S, Mann PC (2019) Spontaneous cholangiofibrosis in a wistar rat. Toxicol Pathol 47(4):556–560

Dei Cas M, Ghidoni R (2019) Dietary curcumin: correlation between bioavailability and health potential. Nutrients 11:9

Dolcet X, Llobet D, Pallares J, Matias-Guiu X (2005) NF-κB in development and progression of human cancer. Virchows Arch 446(5):475–482

Guest RV, Boulter L, Dwyer BJ, Forbes SJ (2017) Understanding liver regeneration to bring new insights to the mechanisms driving cholangiocarcinoma. NPJ Regen Med 2:13

Higashi T, Friedman SL, Hoshida Y (2017) Hepatic stellate cells as key target in liver fibrosis. Adv Drug Deliv Rev 121:27–42

IARC (2012) A review of human carcinogens: *Opisthorchis viverrini* and *Clonorchis sinensis*. IARC Monogr Eval Carcinog Risks Hum 100B:341–370

Ipar VS, Dsouza A, Devarajan PV (2019) Enhancing curcumin oral bioavailability through nanoformulations. Eur J Drug Metab Pharmacokinet 44(4):459–480

Jantawong C, Priprem A, Intuyod K, Pairojkul C, Pinlaor P, Waraasawapati S et al (2021) Curcumin-loaded nanocomplexes: acute and chronic toxicity studies in mice and hamsters. Toxicol Rep 8:1346–1357

Kawanishi S, Hiraku Y, Pinlaor S, Ma N (2006) Oxidative and nitrative DNA damage in animals and patients with inflammatory diseases in relation to inflammation-related carcinogenesis. Biol Chem 387(4):365–372

Khoontawad J, Intuyod K, Rucksaken R, Hongsrichan N, Pairojkul C, Pinlaor P et al (2018) Discovering proteins for chemoprevention and chemotherapy by curcumin in liver fluke infection-induced bile duct cancer. PLoS ONE 13(11):e0207405

Lee JH, Rim HJ, Sell S (1997) Heterogeneity of the "oval-cell" response in the hamster liver during cholangiocarcinogenesis following *Clonorchis sinensis* infection and dimethylnitrosamine treatment. J Hepatol 26(6):1313–1323

Leelawat K, Narong S, Udomchaiprasertkul W, Wannaprasert J, Treepongkaruna SA, Subwongcharoen S et al (2012) Prognostic relevance of circulating CK19 mRNA in advanced malignant biliary tract diseases. World J Gastroenterol 18(2):175–181

Liu W, Zhai Y, Heng X, Che FY, Chen W, Sun D et al (2016) Oral bioavailability of curcumin: problems and advancements. J Drug Target 24(8):694–702

Mahran RI, Hagras MM, Sun D, Brenner DE (2017) Bringing curcumin to the clinic in cancer prevention: a review of strategies to enhance bioavailability and efficacy. AAPS J 19(1):54–81

Mansouri K, Rasoulpoor S, Daneshkhah A, Abolfathi S, Salari N, Mohammadi M et al (2020) Clinical effects of curcumin in enhancing cancer therapy: a systematic review. BMC Cancer 20(1):791

Michalopoulos GK, Bhushan B (2021) Liver regeneration: biological and pathological mechanisms and implications. Nat Rev Gastroenterol Hepatol 18(1):40–55

Mitacek EJ, Brunnemann KD, Suttajit M, Martin N, Limsila T, Ohshima H et al (1999) Exposure to *N*-nitroso compounds in a population of high liver cancer regions in Thailand: volatile nitrosamine (VNA) levels in Thai food. Food Chem Toxicol 37(4):297–305

Narama I, Imaida K, Iwata H, Nakae D, Nishikawa A, Harada T (2003) A review of nomenclature and diagnostic criteria for proliferative lesions in the liver of rats by a working group of the Japanese society of toxicologic pathology. J Toxicol Pathol 16:1–17

Ozaki K, Terayama Y, Matsuura T (2021) Spontaneous cholangiofibrosis adjacent to a dilated common bile duct with intestinal metaplasia in a royal college of surgeons rat. J Toxicol Pathol 34(4):339–343

Pinlaor S, Sripa B, Ma N, Hiraku Y, Yongvanit P, Wongkham S et al (2005) Nitrative and oxidative DNA damage in intrahepatic cholangiocarcinoma patients in relation to tumor invasion. World J Gastroenterol 11(30):4644–4649

Pinlaor S, Yongvanit P, Prakobwong S, Kaewsamut B, Khoontawad J, Pinlaor P et al (2009) Curcumin reduces oxidative and nitrative DNA damage through balancing of oxidant-antioxidant status in hamsters infected with *Opisthorchis viverrini*. Mol Nutr Food Res 53(10):1316–1328

Pinlaor S, Prakobwong S, Hiraku Y, Pinlaor P, Laothong U, Yongvanit P (2010) Reduction of periductal fibrosis in liver fluke-infected hamsters after long-term curcumin treatment. Eur J Pharmacol 638(1–3):134–141

Pinlaor S, Jantawong C, Intuyod K, Sirijindalert T, Pinlaor P, Pairojkul C et al (2021) Solid dispersion improves release of curcumin from nanoparticles: potential benefit for intestinal absorption. Mater Today Commun 26:1–9

Prakobwong S, Yongvanit P, Hiraku Y, Pairojkul C, Sithithaworn P, Pinlaor P et al (2010) Involvement of MMP-9 in peribiliary fibrosis and cholangiocarcinogenesis via Rac1-dependent DNA damage in a hamster model. Int J Cancer 127(11):2576–2587

Prakobwong S, Gupta SC, Kim JH, Sung B, Pinlaor P, Hiraku Y et al (2011a) Curcumin suppresses proliferation and induces apoptosis in human biliary cancer cells through modulation of multiple cell signaling pathways. Carcinogenesis 32(9):1372–1380

Prakobwong S, Khoontawad J, Yongvanit P, Pairojkul C, Hiraku Y, Sithithaworn P et al (2011b) Curcumin decreases cholangiocarcinogenesis in hamsters by suppressing inflammation-mediated molecular events related to multistep carcinogenesis. Int J Cancer 129(1):88–100

Prueksapanich P, Piyachaturawat P, Aumpansub P, Ridtitid W, Chaiteerakij R, Rerknimitr R (2018) Liver fluke-associated biliary tract cancer. Gut Liver 12(3):236–245

Rafiee Z, Nejatian M, Daeihamed M, Jafari SM (2019) Application of different nanocarriers for encapsulation of curcumin. Crit Rev Food Sci Nutr 59(21):3468–3497

Rasyid A, Rahman AR, Jaalam K, Lelo A (2002) Effect of different curcumin dosages on human gall bladder. Asia Pac J Clin Nutr 11(4):314–318

Razavi BM, Ghasemzadeh Rahbardar M, Hosseinzadeh H (2021) A review of therapeutic potentials of turmeric (curcuma longa) and its active constituent, curcumin, on inflammatory disorders, pain, and their related patents. Phytother Res 35(12):6489–6513

Ribeiro AJ, de Souza FRL, Bezerra J, Oliveira C, Nadvorny D, de La Roca Soares MF et al (2016) Gums' based delivery systems: review on cashew gum and its derivatives. Carbohydr Polym 147:188–200

Salyers AA, Vercellotti JR, West SE, Wilkins TD (1977) Fermentation of mucin and plant polysaccharides by strains of bacteroides from the human colon. Appl Environ Microbiol 33(2):319–322

Sato K, Marzioni M, Meng F, Francis H, Glaser S, Alpini G (2019) Ductular reaction in liver diseases: pathological mechanisms and translational significances. Hepatology 69(1):420–430

Shehzad A, Wahid F, Lee YS (2010) Curcumin in cancer chemoprevention: molecular targets, pharmacokinetics, bioavailability, and clinical trials. Arch Pharm 343(9):489–499

Shin HR, Oh JK, Masuyer E, Curado MP, Bouvard V, Fang YY et al (2010) Epidemiology of cholangiocarcinoma: an update focusing on risk factors. Cancer Sci 101(3):579–585

Sirica AE, Gores GJ, Groopman JD, Selaru FM, Strazzabosco M, Wei Wang X et al (2019) Intrahepatic cholangiocarcinoma: continuing challenges and translational advances. Hepatology 69(4):1803–1815

Sriamporn S, Pisani P, Pipitgool V, Suwanrungruang K, Kamsa-ard S, Parkin DM (2004) Prevalence of *Opisthorchis viverrini* infection and incidence of cholangiocarcinoma in khon kaen Northeast Thailand. Trop Med Int Health 9(5):588–594

Srikaeo K, Laothongsan P, Lerdluksamee C (2018) Effects of gums on physical properties, microstructure and starch digestibility of dried-natural fermented rice noodles. Int J Biol Macromol 109:517–523

Sripa B, Tangkawattana S, Brindley PJ (2018) Update on pathogenesis of opisthorchiasis and cholangiocarcinoma. Adv Parasitol 102:97–113

Suwannateep N, Banlunara W, Wanichwecharungruang SP, Chiablaem K, Lirdprapamongkol K, Svasti J (2011) Mucoadhesive curcumin nanospheres: biological activity, adhesion to stomach mucosa and release of curcumin into the circulation. J Control Release 151(2):176–182

Taheri A, Jafari SM (2019) Gum-based nanocarriers for the protection and delivery of food bioactive compounds. Adv Colloid Interface Sci 269:277–295

Thamavit W, Kongkanuntn R, Tiwawech D, Moore MA (1987) Level of *Opisthorchis* infestation and carcinogen dose-dependence of cholangiocarcinoma induction in syrian golden hamsters. Virchows Arch B Cell Pathol Incl Mol Pathol 54(1):52–58

Thamavit W, Pairojkul C, Tiwawech D, Shirai T, Ito N (1994) Strong promoting effect of *Opisthorchis viverrini* infection on dimethylnitrosamine-initiated hamster liver. Cancer Lett 78(1–3):121–125

Thoolen B, Maronpot RR, Harada T, Nyska A, Rousseaux C, Nolte T et al (2010) Proliferative and nonproliferative lesions of the rat and mouse hepatobiliary system. Toxicol Pathol 38(7 Suppl):5S-81S

van Tong H, Brindley PJ, Meyer CG, Velavan TP (2017) Parasite infection, carcinogenesis and human malignancy. EBioMedicine 15:12–23

Vijayakumar EC, Bhatt LK, Prabhavalkar KS (2019) High mobility group box-1 (HMGB1): a potential target in therapeutics. Curr Drug Targets 20(14):1474–1485

Wang C, Nie H, Li K, Zhang YX, Yang F, Li CB et al (2012) Curcumin inhibits HMGB1 releasing and attenuates concanavalin A-induced hepatitis in mice. Eur J Pharmacol 697(1–3):152–157

Wang Y, Wang L, Zhu X, Wang D, Li X (2016) Choleretic activity of turmeric and its active ingredients. J Food Sci 81(7):H1800-1806

Waraasawapati S, Deenonpoe R, Sa-ngiamwibool P, Chamgramol Y, Pairojkul C (2021) Fluke-associated cholangiocarcinoma: a regional epidemic. In: Tabibian JH (ed) Diagnosis and management of cholangiocarcinoma. Springer, Switzerland, pp 265–289

Wierstra I (2013) FOXM1 (forkhead box M1) in tumorigenesis: overexpression in human cancer, implication in tumorigenesis, oncogenic functions, tumor-suppressive properties, and target of anticancer therapy. Adv Cancer Res 119:191–419

Yongvanit P, Pinlaor S, Bartsch H (2012) Oxidative and nitrative DNA damage: key events in opisthorchiasis-induced carcinogenesis. Parasitol Int 61(1):130–135

Zhang JR, Lu F, Lu T, Dong WH, Li P, Liu N et al (2014) Inactivation of FoxM1 transcription factor contributes to curcumin-induced inhibition of survival, angiogenesis, and chemosensivity in acute myeloid leukemia cells. J Mol Med 92(12):1319–1330

Zhang Y, Rauf Khan A, Fu M, Zhai Y, Ji J, Bobrovskaya L et al (2019) Advances in curcumin-loaded nanopreparations: improving bioavailability and overcoming inherent drawbacks. J Drug Target 27(9):917–931

Zhuo JY, Lu D, Tan WY, Zheng SS, Shen YQ, Xu X (2020) CK19-positive hepatocellular carcinoma is a characteristic subtype. J Cancer 11(17):5069–5077

Publisher's Note

Springer Nature remains neutral with regard to jurisdictional claims in published maps and institutional affiliations.